Available online at www.sciencedirect.com
ScienceDirect
Journal of the European Ceramic Society 31 (2011) 3145–3152
www.elsevier.com/locate/jeurceramsoc

Piezoelectric properties and microstructures of ZnO-doped $Bi_{0.5}Na_{0.5}TiO_3$ ceramics

Ying-Chieh Lee [a,*], Tai-Kuang Lee [b], Jhen-Hau Jan [a]

[a] Department of Materials Engineering National Pingtung University of Technology and Science, Taiwan, ROC
[b] Department of Electrical Engineering, National Cheng Kung University, Tainan 701, Taiwan, ROC

Available online 31 May 2011

Abstract

This article studies the microstructure and piezoelectric properties of a ceramic lead-free NBT under different amount of ZnO doping. X-ray diffraction shows that Zn^{2+} diffuses into the lattice of $(Bi_{0.5}Na_{0.5})TiO_3$ to form a solid solution with a pure perovskite structure. By modifying the zinc oxide content, the sintering behavior of $(Bi_{0.5}Na_{0.5})TiO_3$ ceramics was significantly improved and the grain size was increased. The piezoelectric coefficient d_{33} for the 1.0 wt.% ZnO-doped $(Bi_{0.5}Na_{0.5})TiO_3$ ceramics sintered at 1050 °C was found to be 95 pC/N, and the electromechanical coupling factor $k_p = 0.13$. However, the piezoelectric coefficient d_{33} for the 0.5 wt.% ZnO-doped $(Bi_{0.5}Na_{0.5})TiO_3$ ceramics sintered at 1140 °C was found to be 110 pC/N, and the electromechanical coupling factor $k_p = 0.17$.

Keywords: Piezoelectricity; Microstructure; Dielectric properties; Ferroelectricity

1. Introduction

$Pb(Zr_xTi_{1-x})O_3$ (PZT) ceramics possess excellent piezoelectric properties. However, the production of PZT-based ceramics is not environmentally friendly because of PbO evaporation during the firing process. It is necessary to develop high-performance lead-free piezoelectric materials if the environmental damage associated with the production of PZT is to be prevented.[1–3] For example, barium titanate ($BaTiO_3$), a typical lead-free piezoelectric material, is generally used for piezoelectric applications such as sonar.[4] This ceramic has a relatively high electromechanical coupling factor. However, it possesses a low Curie temperature ($T_c = 130$ °C) which limits its range of working temperature.[5] Bismuth potassium titanate $(Bi_{0.5}K_{0.5})TiO_3$ (KBT) ceramics, on the other hand, were only recently discovered to potentially be useful for specific applications. However, it is difficult to obtain the desired structure of KBT using conventional ceramic fabrication techniques.[6,7]

Bismuth sodium titanate $(Bi_{0.5}Na_{0.5})TiO_3$ (NBT) is quite possibly an excellent potential replacement for lead-containing piezoelectric ceramics. It has a high Curie temperature (T_c) of 320 °C, and a ferroelectric to antiferroelectric phase transition point (T_c) of 200 °C, as well as relatively large remnant polarization (P_r) of 38 μC/cm^2 and a coercive field (E_c) of 73 kV/cm.[5,8–11] However, NBT still cannot replace PZT-based ceramics due to its large coercive field and high conductivity. Recently, many researchers have studied the effects of doping NBT ceramics with small amounts of Ba, Ca, Pb, Sr, Se, Zr, La, K or Bi.[12–16] Adding dopants to NBT ceramics can lower both the coercive field and conductivity. However, the piezoelectric properties of NBT are still not comparable to PZT.

In this paper, NBT based piezoelectric ceramics doped with ZnO were synthesized using a conventional solid state reaction. The mechanism through which Zn doping altered the piezoelectric properties and microstructures of NBT ceramics was investigated and discussed.

2. Experimental procedure

$Na_{0.5}Bi_{0.5}TiO_3$ ceramic samples were prepared using a solid-state reaction method. Reagent grade powders (Alfa Aesar) of Na_2CO_3 (99.997%), Bi_2O_3 (99.975%) and TiO_2 (99.99%) were mixed in stoichiometric amounts to produce starting materials for preparing the ceramics. The carbonates were dried at 200 °C for 2 h before mixing so as to remove any water content. The mixtures of powders were homogenized using a mortar and pestle with added ethanol as a medium. The mixture was then milled

* Corresponding author. Tel.: +886 8 7703202; fax: +886 8 7740552.
E-mail address: YCLee@mail.npust.edu.tw (Y.-C. Lee).

0955-2219/$ – see front matter © 2011 Elsevier Ltd. All rights reserved.
doi:10.1016/j.jeurceramsoc.2011.05.010

with ethanol in a planetary ball mill at 90 rpm for 24 h using yttria-stabilized zirconia balls. The milled powders were dried and calcined at 800 °C for 2 h in air, then crushed into a powder. An appropriate amount of ZnO was mixed with the NBT powders using the same procedure. The powders were mixed with a binder (polyvinyl alcohol; PVA) additive and then were pressed into disk-shaped specimens. The pellets were then sintered in air at temperatures ranging from 1000 °C to 1140 °C for a period of 4 h with a heating and cooling rate of 5 °C/min.

The crystalline phases of the sintered ceramics were identified by X-ray diffraction pattern analysis (XRD, Bruker D8A, Germany) using Cu-Kα radiation for 2θ from 20 to 80°. The diffraction spectra were collected at a scan rate of 2.5°/min. The DIFFRAC plus TOPAS version 3.0 program was used to determine the lattice parameters. Microstructural observation of the sintered ceramics was performed using a scanning electron microscope (SEM, JEOL. JEL-6400 Japan) equipped with energy-dispersive spectroscopy (EDS). The bulk density of the sintered pellets was measured using the Archimedes method. Particle size was measured using a particle size analyzer (Malvern, Mastersizer 2000, UK). In order to measure the dielectric, ferroelectric and piezoelectric properties, different sizes of capacitors were made by applying silver electrodes on both sides of the pellets, drying, and then firing at 800 °C for 10 min. The capacitance and dielectric losses of the samples were measured at 1 kHz in room temperature using an LCR meter (Agilent 4284A; Agilent Technologies, Inc., Santa Clara, CA) and a chamber furnace. The dielectric constants were calculated from the measured values of the capacitance (C_p). Prior to measuring the piezoelectricity of the samples they were poled in silicon oil in an electric field of 6 kV/mm at a temperature of 70 °C for 15 min. A piezometer (PiezoMeter System Quite-static d_{33} meter, ZJ-3AN, CH) was then used to measure the d_{33} piezoelectric coefficient at room temperature and at constant frequency of 100 Hz.

3. Results and discussion

3.1. Phase evolution in the sintered ceramics

XRD patterns of the ZnO doped NBT ceramics sintered at 1050 °C and 1140 °C are given in Figs. 1 and 2, respectively. These results show that all the samples are composed of a single phase for compositions doped with between 0.0 (pure NBT) and 1.0 wt.% ZnO and sintered at 1050 °C or 1140 °C. It is clear that all specimens exhibit typical ABO_3 perovskite diffraction peaks at room temperature and no second phases were detected when the amount of ZnO dopant was 1 wt.%. This implies that Zn^{2+} has entered into the crystalline lattice within the NBT ceramic to form a homologous solid solution. The presence of minor impurity phases such as Zn_2TiO_4 was detected for samples with ZnO dopant ≥2.0 wt.%, this is shown in Figs. 1d and e and 2d and e. The diffraction patterns of NBT were indexed as rhombohedral (ICDD-PDF #36-0340), however that of NBT is composed of main peaks without any separation. Thus, NBT shows pseudo-cubic symmetry in crystal structure (ICDD-PDF #89-3109).[17,18] Watcharapasorn et al.[19] reported that all NBT ceramic samples

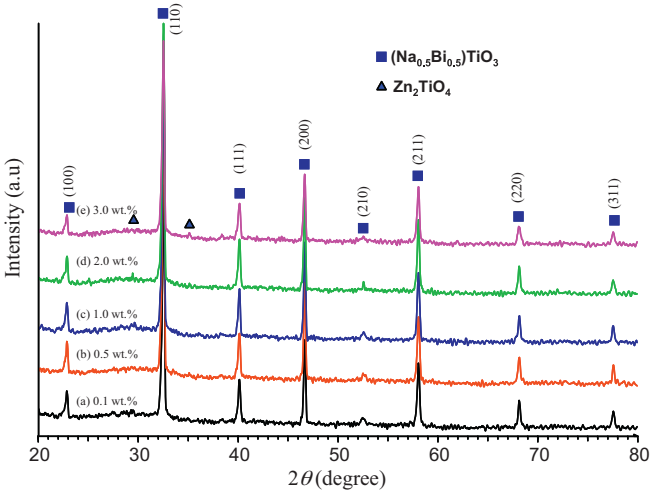

Fig. 1. X-ray diffraction spectra of $Na_{0.5}Bi_{0.5}TiO_3$ ceramics sintered at 1050 °C with different amounts of ZnO dopant.

were virtually single phase with rhombohedral structure. The peak splitting due to rhombohedral symmetry was difficult to observed in this compound since peak overlapping occurred and it was known that its lattice dimension was nearly cubic.[20]

The comparison between the XRD patterns of ZnO doped NBT ceramics in Figs. 1 and 2 shows that there is significantly more Zn_2TiO_4 phase present for NBT ceramics with ZnO dopant (≥2.0 wt.%) sintered at 1140 °C compared to those sintered at 1050 °C. However, XRD is not sensitive enough to identify low volume fractions of a secondary phase; further study of the microstructure using transmission and scanning electron microscopy was used to be discussed later in this article.

Fig. 3 shows the variation in the lattice parameter "a" and angle "α" as a function of the addition of ZnO for NBT sintered at 1140 °C. Increasing the levels of ZnO results in a significant increase in the lattice constant to a maximum at ZnO = 1.0 wt.%, and then a rapid decrease. The value of the lattice parameter "a" was found to increase with increasing Zn concentration over the range of 0–1 wt.% until the concentration reached stoichiome-

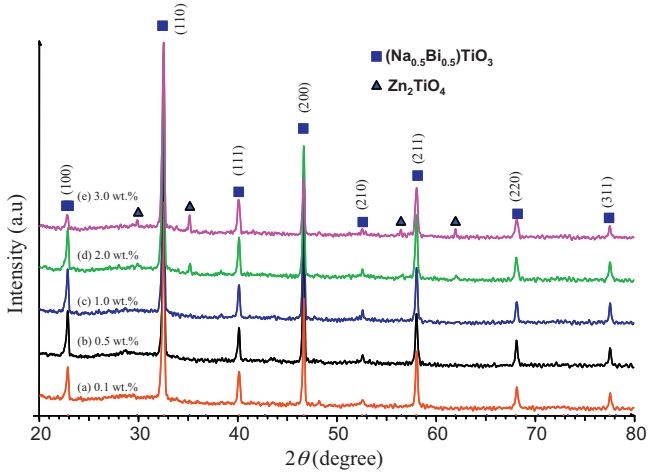

Fig. 2. X-ray diffraction spectra of $Na_{0.5}Bi_{0.5}TiO_3$ ceramics sintered at 1140 °C with different amounts of ZnO dopant.

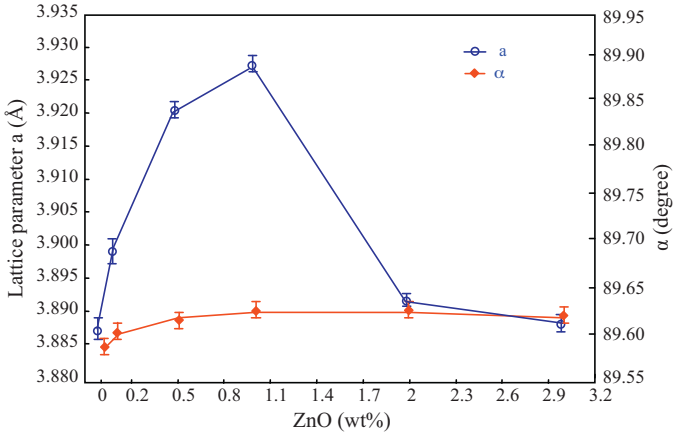

Fig. 3. The variation of lattice parameter and angle α with addition of ZnO into $Na_{0.5}Bi_{0.5}TiO3$ ceramics sintered at 1140 °C. The error bar indicates standard deviation.

try. This may be attributed to the ionic radius of Zn^{2+} (0.74 Å), which is larger than that of Ti^{4+} (0.605 Å).[21] When Zn is substituted into Ti sites within the perovskite ABO_3 structure, it will create lattice strain and oxygen vacancies, thereby increasing the lattice parameter. Roth et al.[22] reported that $BaTiO_3$ accepted less than 2 mol% of ZnO in solid solution in the system ZnO–$BaTiO_3$. For system ZnO–$Bi_{0.5}Na_{0.5}TiO_3$, 1 wt.% ZnO equals to 2.56 mol% ZnO. Therefore, the experimental results indicate that the solubility limit of Zn in NBT ceramics is below 1.0 wt.%. In Fig. 3, the α initially increases slightly to a maximum at ZnO = 1.0 wt.%, then keeps a constant until 3 wt.% ZnO.

In an ideal cubic perovskite ABO_3, the coordination numbers of the A and B sites are 12 and 6, respectively, and $t = 0.77–1.1$. The tolerance factor (t) is a concept for the arrangement of interpenetrating dodecahedra and octahedra in a ABO_3 perovskite structure introduced by Goldschmidt,[23] which is given by,

$$t = \frac{R_A + R_B}{\sqrt{2}\,(R_B + R_O)}$$

where R_A, R_B, and R_O are the ionic radii of cation A, B and oxygen, respectively. The ionic radii of Bi, Na, Ti, O, and Zn are summarized as follows: A site (12 coordinate): $Bi^{3+} = 1.4$ Å, $Na^{+} = 1.39$ Å; B site (six coordinate): $Zn^{2+} = 0.74$ Å, $Ti^{4+} = 0.605$ Å, $O^{2-} = 1.4$ Å. For complex perovskite system, R_A and R_B are the ionic radii of composed ions normalized by the atomic ratio. For the example of $(Bi_{0.5}Na_{0.5})TiO_3$, $R_A = 0.5 \times 1.4$ Å $+ 0.5 \times 1.39$ Å $= 1.395$ Å, $R_B = 0.605$ Å, $R_O = 1.40$ Å, so that t is 0.9857.

On the other hand, Zn^{2+} would occupy the B-sites within the perovskite structure because Zn^{2+} is too small for the A site. When Zn^{2+} is substituted into the B site, a doubly ionized oxygen vacancy is formed,

$$ZnO \rightarrow Zn_{Ti}'' + V_{\ddot{O}} + O_O \quad (1)$$

Charged oxygen vacancies, in combination with Zn ions, obviously give rise to local deformation within perovskite unit cells. Moreover, both electric dipoles formed from Zn_{Ti}''–$V_{\ddot{O}}$ complexes and elastic dipoles as a result of distortions caused by VO will be present in the doped NBT ceramics. Oxygen vacancies in ZnO-doped NBT residing at the corners of the octahedra are well interconnected, and can therefore be regarded as rel-

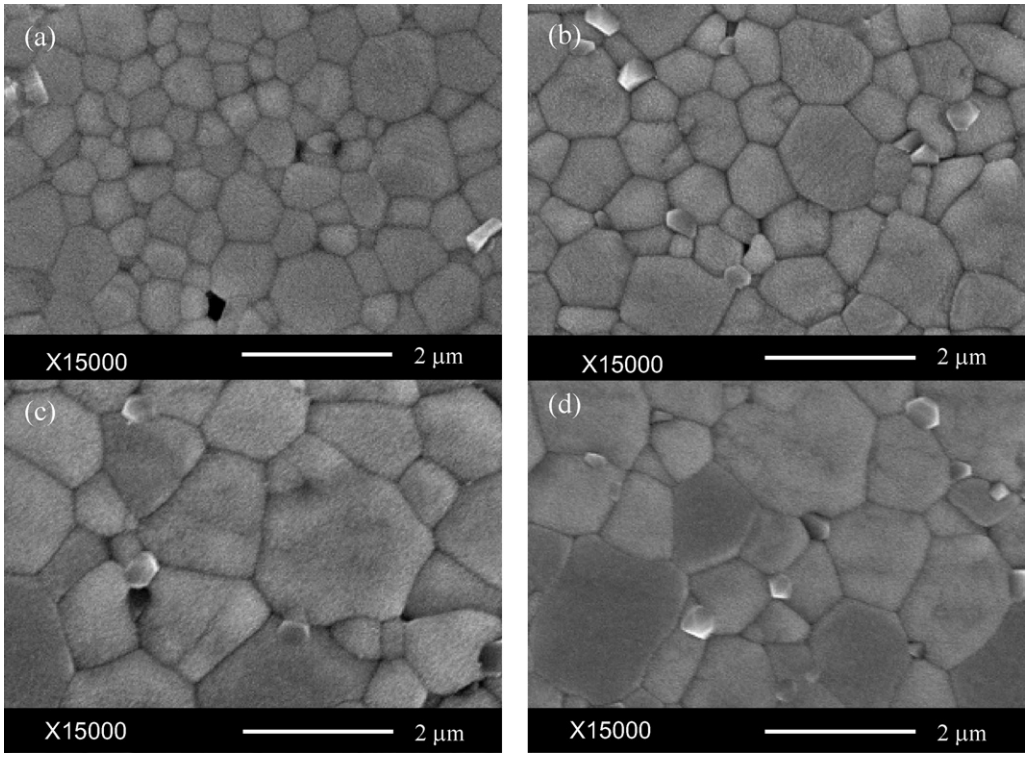

Fig. 4. SEM of $Na_{0.5}Bi_{0.5}TiO_3$ ceramics sintered at 1050 °C with a ZnO composition of: (a) 0 wt.%; (b) 0.5 wt.%; (c) 1 wt.%; and (d) 3 wt.%.

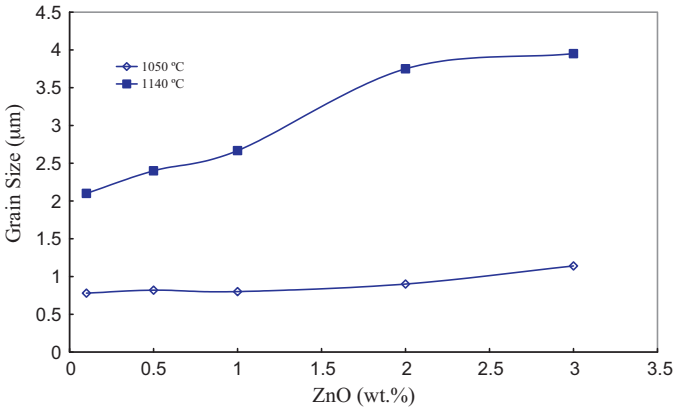

Fig. 5. Grain size of ZnO doped $Na_{0.5}Bi_{0.5}TiO_3$ ceramics sintered at 1050 °C and 1140 °C, respectively.

atively "mobile". Mobile defect complexes migrate to domain boundaries, in a similar way to those reported in hard ferroelectric Mg-doped BST.[24] According to Chan et al.,[25] the presence of VO in acceptor-doped materials allows for the incorporation of excess O_2.

SEM micrographs of the NBT specimens sintered at 1050 °C with 0, 0.5, 1.0, and 3.0 wt.% of ZnO are shown in Fig. 4a–d, respectively. The images show that significant densification of NBT ceramics with ZnO dopant occurred. It is widely accepted that pure NBT ceramic has to be sintered at 1150 °C for several hours. Therefore these results show that a small amount of ZnO dopant can increase the density of NBT ceramics at 1050 °C. These SEM images confirm that the ceramics are sintered to a high density. The relative density of NBT ceramics is discussed below. Fig. 5 shows that increasing the amount of ZnO dopant within the NBT increases the grain size after sintering. The grain sizes of specimens sintered at 1050 °C with 0.1, 0.5, 1, 2 and 3 wt.% ZnO addition are 0.78, 0.82, 0.80, 0.90 and 1.14 μm, respectively. The grain sizes of specimens sintered at 1140 °C with 0.1, 0.5, 1, 2 and 3 wt.% ZnO addition are 2.1, 2.4, 2.67, 3.75 and 3.95 μm, respectively. Additionally, the grain size of NBT ceramics significantly increased when the specimens were sintered at a higher temperature (1140 °C). The results show that ZnO promotes grain growth within NBT. The possible reasons for the grain growth are as follows: Zn^{2+} enters into B-site of the perovskite structure to substitute for Ti^{4+} due to their matching radii. To maintain overall electrical neutrality, oxygen vacancies are created. As is generally recognized, the presence of oxygen vacancies is beneficial to mass transport during sintering. This is assumed to be responsible for the promoted grain growth as the content of ZnO increases.[19] SEM micrographs of the NBT specimens doped with 1.0 wt.% ZnO and sintered at different temperatures are shown in Fig. 6a–d. The microstructures of the sintered ceramics were significantly different. The results show that the grain size of the specimen increased with sintering temperature.

For NBT ceramics containing 3 wt.% ZnO and sintered at 1140 °C, we observed a microstructure with a significant amount of trapezium-like grains. This is shown in Fig. 7a and b. According to the XRD spectra in Fig. 2, the composition of the

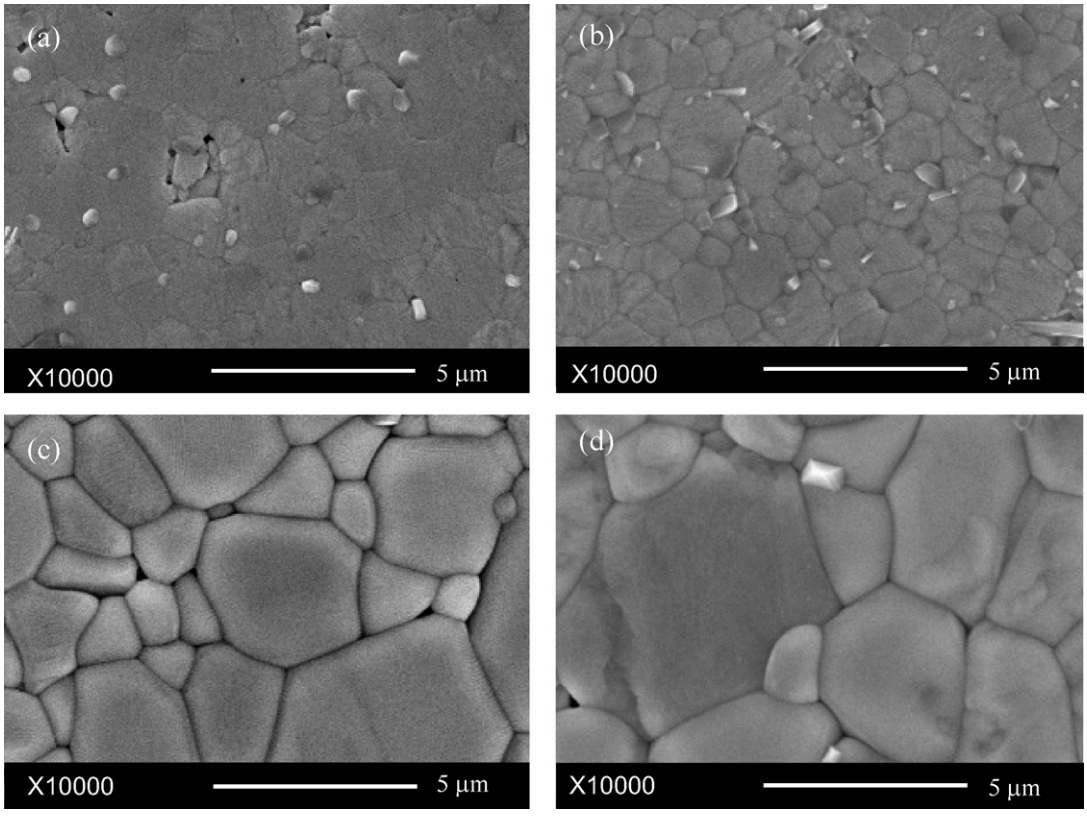

Fig. 6. SEM of $Na_{0.5}Bi_{0.5}TiO_3$ ceramics with 1 wt.% ZnO dopant sintered at: (a) 1000 °C; (b) 1050 °C; (c) 1100 °C; and (d) 1140 °C.

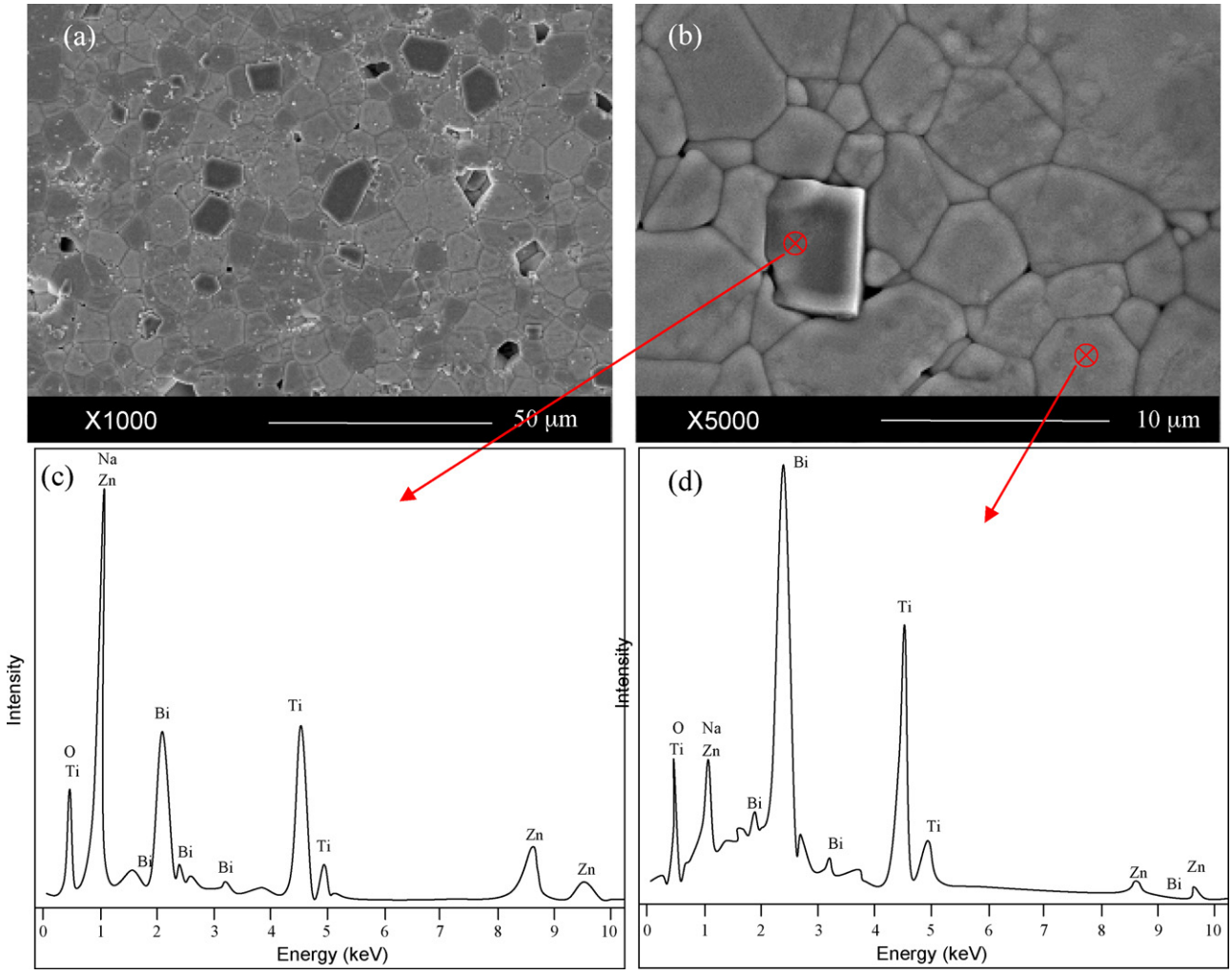

Fig. 7. $Na_{0.5}Bi_{0.5}TiO_3$ ceramics sintered at 1140 °C with 3 wt.% ZnO addition: (a) 1000× morphology; (b) 5000× morphology; (c) EDS analysis of second phase; (d) EDS analysis of matrix.

secondary phase should be Zn_2TiO_4 for NBT with a ZnO content ≥2 wt.%. Energy dispersive spectroscopy (EDS) was used to investigate the secondary phases within the NBT ceramic doped with 3 wt.% ZnO and sintered at 1140 °C. These results are presented in Fig. 7c and d. In comparison to the matrix phase (Fig. 7d), the trapezium-like grains have higher Zn signal intensities (Fig. 7c). Considering that the X-ray diffraction results clearly show that the formation of the Zn_2TiO_4 phase was preferred when the ZnO was ≥2 wt.%, we therefore conclude that the square-like grains are composed of Zn_2TiO_4. The reaction can be expressed as follows:

$$2ZnO + TiO_2 \rightarrow Zn_2TiO_4 \quad (3)$$

In order to further study the secondary phase, samples doped with 3 wt.% ZnO and sintered at 1140 °C were prepared for TEM microstructural analysis. The TEM image and EDX analysis of NBT with 3.0 wt.% ZnO addition are shown in Fig. 8. Fig. 8a shows the presence of two phases that can be attributed to liquid sintering. The second phase is located at the triple-junctions of NBT grains. TEM–EDX analysis shows that, compared to the matrix phase (Fig. 8b), the second phase has higher Zn signal intensity (Fig. 8c), and smaller Bi, Na and Ti signal intensity. Therefore, the second phase is Zn-rich.

3.2. Density and piezoelectric properties of the sintered ceramics

NBT ceramics with different amounts of ZnO doping were sintered in air at temperatures ranging from 1000 to 1140 °C for 4 h. The particle size of the starting powder was 0.5 ± 0.1 μm in all experiments. Fig. 9 shows the bulk density of the NBT ceramics as a function of sintering temperature and ZnO doping. For samples doped with between 0.1 and 0.5 wt.% ZnO the density of the NBT ceramics increased at higher sintering temperatures and reached a maximum when sintered above 1100 °C. The theoretical density of the $Na_{0.5}Bi_{0.5}TiO_3$ ceramics is approximately 5.87 g/cm^3.[26] For samples with ZnO doped at between 1.0 and 3.0 wt.%, NBT ceramics can be sintered to over 98% of the theoretical density (i.e. 5.76 g/cm^3, at 1000 °C for 4 h) at temperatures as low as 1000 °C. The influence of sintering temperature on the density of the NBT ceramics depends on the amount of ZnO addition. The sintering temperature of NBT can

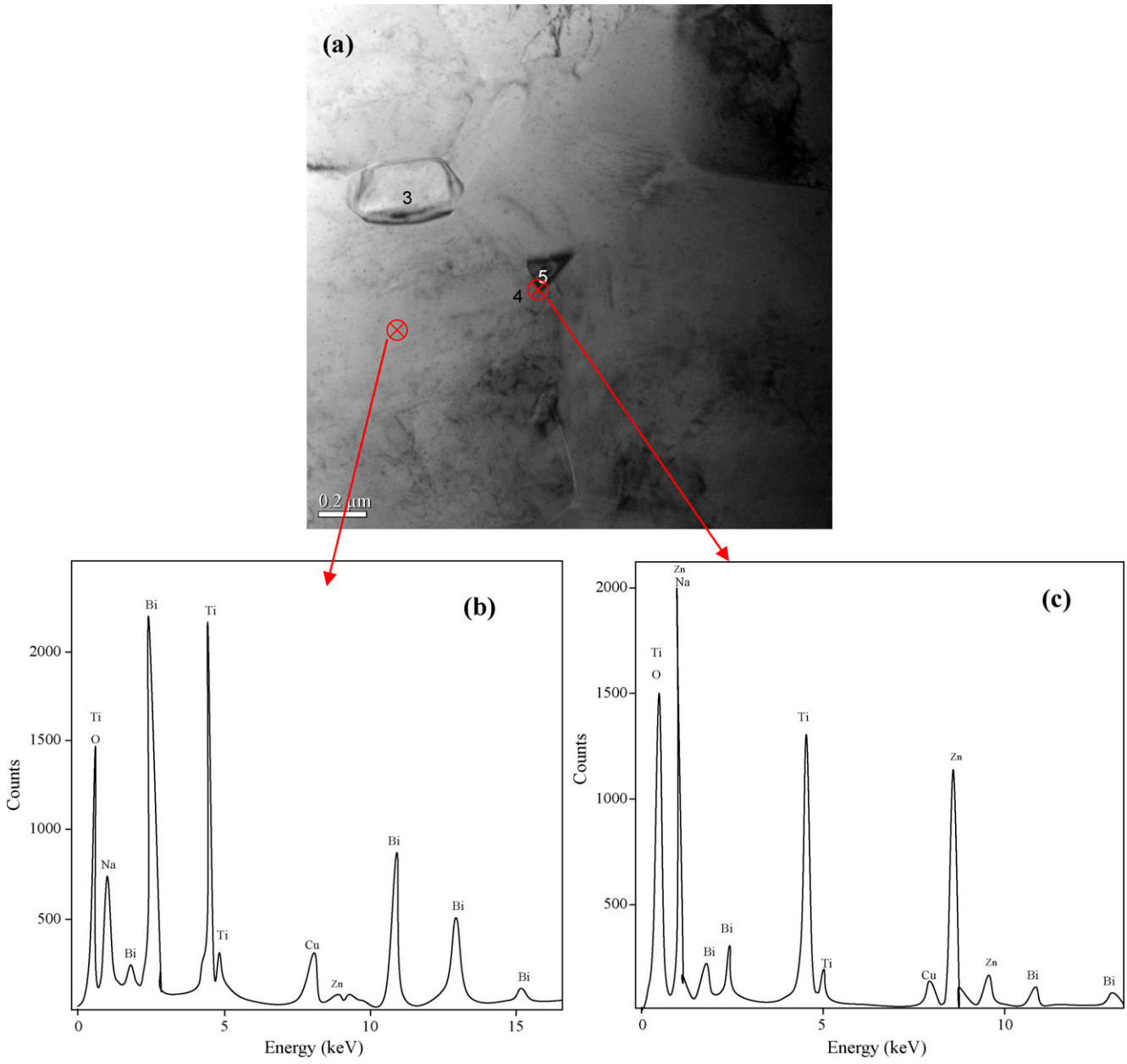

Fig. 8. Microstructure of the $Na_{0.5}Bi_{0.5}TiO_3$ ceramic with 3.0 wt.% ZnO dopant sintered at 1140 °C for 2 h as observed by transmission electron microscopy: (a) morphology; (b) energy-dispersive spectroscopy (EDS) of the secondary phase; and (c) EDS of the matrix.

be reduced to ~1000 °C by increasing the ZnO sintering aids. However, pure NBT ceramic has to be sintered at ~1150 °C for several hours,[3] therefore a small amount of ZnO addition can increase the density of NBT ceramics sintered at 1000 °C. This result indicates that the ZnO assists in the densification of the NBT ceramics by promoting liquid-phase sintering. It is also interesting to note that the sintered ceramic with the highest relative density is not that with the greatest amount of ZnO. In fact, the addition of 1 wt.% ZnO to the sample sintered at 1050 °C resulted in the highest density achieved. The reason for this is that ZnO in heavily doped samples did not become volatile or form an appropriate amount of the liquid phase. Instead, it remained in the microstructure and formed a secondary phase. According to X-ray diffraction and SEM morphology analysis, the amount of secondary phase Zn_2TiO_4 increased significantly when ZnO was present at higher levels. The Zn_2TiO_4 formed in a spinel cubic structure and had a density of 5.33 g/cm^3.[27] Therefore, the bulk density of the NBT ceramic can be reduced when more Zn_2TiO_4 forms in the samples.

Fig. 10 shows the variation of the piezoelectric constant d_{33} and dielectric constant with respect to the ZnO content and sintering temperature. It has been reported that the piezoelectric constant d_{33} of NBT ceramics made by the conventional solid-state method reaches approximately 58 pC/N.[28] Fig. 10a shows that the d_{33} of NBT with ZnO is apparently larger than dopant free NBT ceramics, and the d_{33} reached 110 pC/N for NBT ceramics with 0.5 wt.% dopant, sintered at 1140 °C. In addition, the d_{33} of NBT with 1.0 wt.% dopant sintered at 1050 °C was

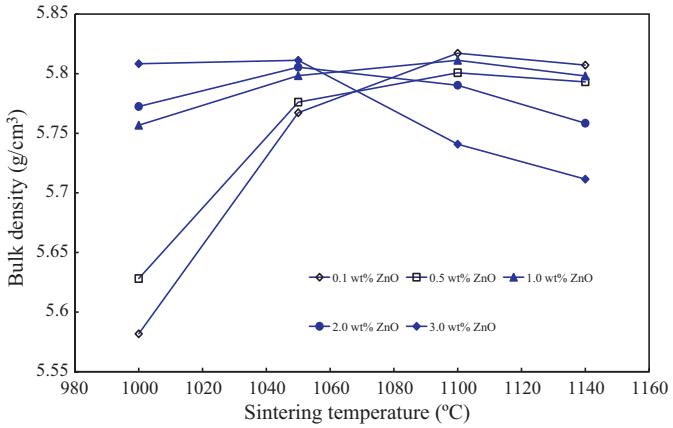

Fig. 9. Bulk density vs sintering temperature of the $Na_{0.5}Bi_{0.5}TiO_3$ ceramics with different ZnO dopant levels.

95 pC/N which is greater than pure NBT sintered at 1150 °C. The radius of Zn^{2+} (0.74 Å) is closer to the radius of Ti^{4+} (0.605 Å). In view of the radius, it is obvious that Zn^{2+} cannot enter into the A-site of NBT perovskite because of the much larger radius of Bi^{3+} (1.4 Å) and Na^{+} (1.39 Å), but it may occupy B-site which has been discussed in Fig. 3. When Zn^{2+} occupies Bi-site, a doubly ionized oxygen vacancy is formed. The lattice deformation can make the ferroelectric domains reorientation easier during electrical poling and lead to the enhancement of piezoelectric properties.[29]

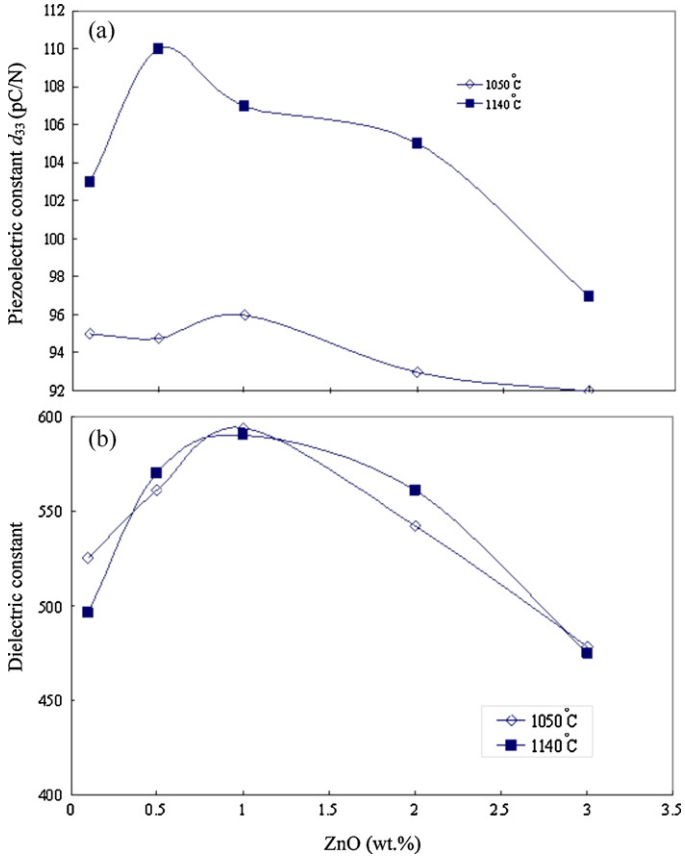

Fig. 10. Dielectric constant and piezoelectric constant d_{33} of ZnO doped $Na_{0.5}Bi_{0.5}TiO_3$ ceramics sintered at 1050 °C and 1140 °C, respectively.

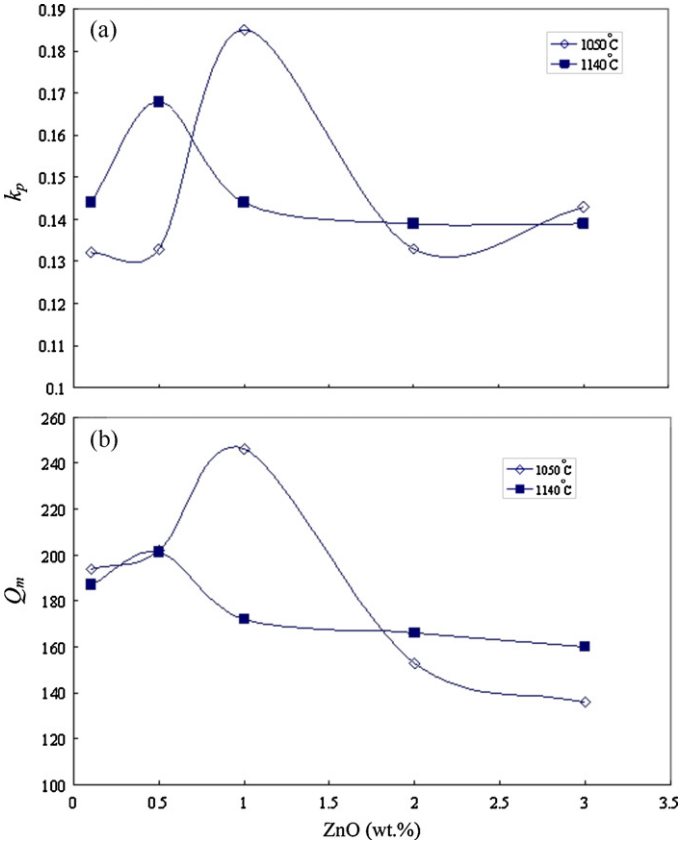

Fig. 11. Planar electro-mechanical coupling factor k_p and mechanical quality factor Q_m of ZnO doped $Na_{0.5}Bi_{0.5}TiO_3$ ceramics sintered at 1050 °C and 1140 °C, respectively.

The dielectric constant (ε_r) of ZnO-doped NBT ceramics as a function of their ZnO content was measured at 1 MHz at ambient temperature. The results are shown in Fig. 10b. The dielectric constants of the samples increased with the amount of ZnO addition, and reached a maximum value at 1.0 wt.% for sintered at either 1050 °C or 1140 °C. The dielectric constant gradually decreased with increasing amounts of ZnO beyond 1.0 wt.%. In addition, the dielectric coefficient of the samples with 1.0 wt.% ZnO and sintered at 1050 °C or 1140 °C were ~594 and ~590, respectively. These values are higher than that of the sample with 2.0 wt.% ZnO (~542 for 1050 °C and ~561 for 1140 °C). Two causes have been identified for the higher ε_r value of the sample with 1.0 wt.% ZnO: (1) no secondary phase and (2) larger lattice strain. Preethi et al.[30] reported that the distortion of the crystalline lattice due to a decrease in the ionic radii of a substitutional solute might be the reason for the increase in dielectric constant. Since Zn acts as an acceptor to replace Ti on the B site of the perovskite ABO_3 structure within the NBT, this leads to a rise in the local deformation of the unit cell and a significant increase in its permittivity. On the other hand, the Zn_2TiO_4 phase has a low dielectric constant, and will contribute to the dielectric constants of its host material according to the J.C. Maxwell equation.[31]

Fig. 11 shows the variation of the planar electro-mechanical coupling factor k_p and mechanical quality factor Q_m with the ZnO content and sintering temperature. The planar

electromechanical coupling factor and mechanical quality factor gradually increase and reach peak values when the doping level of ZnO reached 1.0 wt.% at 1050 °C sintering; the two values decrease sharply with further ZnO doping. Similar curves were observed for NBT sintered at 1140 °C, but the peak value was at a doping level of 0.5 wt.% ZnO. The results show that the addition of ZnO can improve the piezoelectric properties of NBT ceramics significantly.

4. Conclusions

NBT ceramics doped with 0.1–3.0 wt.% ZnO were investigated. There is no obvious change in the crystal structure of NBT ceramics containing ZnO. An X-ray diffraction examination of the products indicates that they consist mainly of a $Na_{0.5}Bi_{0.5}TiO_3$ crystalline phase with Zn_2TiO_4 as a secondary phase. The secondary phase is formed due to the addition of ZnO ($\geq$2 wt.%). The appropriate doping of NBT with ZnO improves the piezoelectric and dielectric properties of NBT ceramics significantly. At room temperature, NBT ceramics sintered at 1140 °C and doped with 0.5 wt.% ZnO show quite good performance: $d_{33} = 110$ pC/N, $k_p = 0.17$, $Q_m = 201$, $\varepsilon_r = 570$ (at a frequency of 1 MHz). Moreover, NBT ceramics with 1.0 wt.% ZnO dopant sintered at 1050 °C exhibit $d_{33} = 95$ pC/N, $k_p = 0.13$, $Q_m = 250$, $\varepsilon_r = 574$ (at a frequency of 1 MHz).

References

1. Cross E. Lead-free at last. *Nature* 2004;**432**:24–8.
2. Saito Y, Takao H, Tani T, Nonoyama T, Takatori K, Homma T, et al. Lead-free piezoceramics. *Nature* 2004;**432**:84–90.
3. Takenaka T, Nagata H. Current status and prospects of lead-free piezoelectric ceramics. *J Eur Ceram Soc* 2005;**25**:2693–700.
4. Walter J, Merz J. The electric and optical behavior of $BaTiO_3$ single domain crystals. *Phys Rev* 1949;**76**:1219–22.
5. Zhoua XY, Gu HS, Wang TY, Li WY, Zhou TS. Piezoelectric properties of Mn-doped $(Na_{0.5}Bi_{0.5})_{0.92}Ba_{0.08}TiO_3$ ceramics. *Mater Lett* 2005;**59**:1649–52.
6. Otonicar M, Skapin SD, Spreitzer M, Suvorov D. Compositional range and electrical properties of the morphotropic phase boundary in the $Na_{0.5}Bi_{0.5}TiO_3$–$K_{0.5}Bi_{0.5}TiO_3$ system. *J Euro Ceram Soc* 2010;**30**:971–9.
7. König J, Spreitzer M, Jančar B, Suvorov D, Samardžija Z, Popovič A. The thermal decomposition of $K_{0.5}Bi_{0.5}TiO_3$ ceramics. *J Eur Ceram Soc* 2009;**29**:1695–701.
8. Smolensky GA, Isupov VA, Agramovskaya AI, Ktainik NN. New ferroelectrics of complex composition. *Sov Phys Solid State* 1961;**2**:2651–7.
9. Buhrer CF. Some properties of bismuth perovskites. *J Chem Phys* 1962;**36**:798–803.
10. Suchanicz J, Kwapulinsk. X-ray diffraction study of the phase transitions in $Na_{0.5}Bi_{0.5}TiO_3$. *J Ferroelectrics* 1995;**165**:249–53.
11. Yet-Ming Chiang, Farrey Gregory W, Soukhojak Andrey N. Ferroelectric, piezoelectric pyroelectric studies on BaTi0.95(Ni1/3Nb2/3)0.05O3 ceramics. *Appl Phys Lett* 1998;**73**:3684–8.
12. Nagata H, Takenaka T. Lead-free piezoelectric ceramics of $(Na_{0.5}Bi_{0.5})TiO_3$–$_{0.5}(Bi_2O_3$–$Sc_2O_3)$ system. *Jpn J Appl Phys* 1997;**36**:6055–7.
13. Soukhojak AN, Wang H, Farrey GW, Chiang Y-M. Superlattice in single crystal barium-doped sodium bismuth titanate. *J Phys Chem Solids* 2000;**61**:301–4.
14. Park S-E, Hong KS. Variations of structure and dielectric properties on substituting A-site cations for Sr^{2+} in $(Na_{1/2}Bi_{1/2})TiO_3$. *J Mater Res* 1997;**12**:2152–7.
15. Sakata K, Masuda Y. Ferroelectric and antiferroelectric properties of $(Na_{0.5}Bi_{0.5})TiO_3$–$SrTiO_3$ solid solution ceramics. *Ferroelectrics* 1974;**7**:347–9.
16. Lee J-K, Yi JY, Hong K-S. Relationship between structure and dielectric property in $(1-x)(Na_{1/2}Bi_{1/2})TiO_3$–$xPbZrO_3$ ceramics. *Jpn J Appl Phys Part 1* 2001;**40**:6003–7.
17. Fan Guifen, Lu Wenzhong, Wang Xiaohong, Liang Fei, Xiao Jianzhong. Phase transition behaviour and electromechanical properties of $(Na_{1/2}Bi_{1/2})TiO_3$–$KNbO_3$ lead-free piezoelectric ceramics. *J Phys D: Appl Phys* 2008;**41**:1–6.
18. Shinjiro Tashiro, Hideki Nagamatsu, Kunihiro Nagata. Sinterability and piezoelectric properties of $KNbO_3$ ceramics after substituting Pb and Na for K. *Jpn J Appl Phys* 2002;**41**:7113–8.
19. Watcharapasorn A, Jiansirisomboon S. Grain growth kinetics in Dy-doped $Bi_{0.5}Na_{0.5}TiO_3$ ceramics. *Ceram Int* 2008;**34**:769–72.
20. Smolenskii GA, Isupov VA, Agranovskaya AI, Kainik NN. New ferroelectrics of complex composition IV. *Sov Phys Solid State (Engl Transl)* 1961;**2**:2651–4.
21. Lee Ying-Chieh, Huang Yen-Lin. Effects of CuO doping on the microstructural and dielectric properties of Ba0.6Sr0.4TiO_3 ceramics. *J Am Ceram Soc* 2009;**92**:2661–7.
22. Roth RS, Rawn CJ, Lindsay CG, Won-Ng W. Phase equilibrium and crystal chemistry of the binary and ternary polytitanates and crystallography of the barium zinc polytitanates. *J Solid State Chem* 1993;**104**:99–118.
23. Muller O, Roy R. *The major ternary structural families*. New York: Springer; 1974. p. 221.
24. Su B, Button TW. Microstructure and dielectric properties of Mg-doped barium strontium titanate ceramics. *J Appl Phys* 2004;**95**:1382–5.
25. Chan NH, Sharma RK, Smyth DM. Nonstoichiometry in acceptor-doped $BaTiO_3$. *J Am Ceram Soc* 1982;**65**:167–70.
26. Ichinose N, Udagawa K. Piezoelectric properties of $(Bi_{1/2}Na_{1/2})TiO_3$ based ceramics. *Ferroelectrics* 1995;**169**:317–25.
27. Shih Chuan-Feng, Li Wei-Min, Lin Ming-Min, Hsiao Chu-Yun, Hung Kuang-Teng. Low-temperature sintered Zn_2TiO_4:TiO_2 with near-zero temperature coefficient of resonant frequency at microwave frequency. *J Alloy Compd* 2009;**485**:408–12.
28. Lee Wei-Chih, Huang Chi-Yuen, Tsao Liang-Kuo, Wu Yu-Chun. Chemical composition and tolerance factor at the morphotropic phase boundary in $(Bi_{0.5}Na_{0.5})TiO_3$-based piezoelectric ceramics. *J Eur Ceram Soc* 2009;**29**:1443–8.
29. Fu Peng, Xu Zhijun, Chu Ruiqing, Li Wei, Zang Guozhong, Hao Jigong. Piezoelectric, ferroelectric and dielectric properties of La_2O_3-doped $(Bi_{0.5}Na_{0.5})_{0.94}Ba_{0.06}TiO_3$ lead-free ceramics. *Mater Des* 2010;**31**:796–801.
30. Preethi TM, Ratheesh R. Synthesis and dielectric properties of a new class of $MX_6Ti_6O_{19}$ (M = Ba, Sr and Ca; X = Mg and Zn) ceramics. *Mater Lett* 2003;**57**:2545–52.
31. Moulson AJ, Herbert JM. *Electroceramics: materials, properties, application*. London: Chapman and Hall; 1990. p. 79–82.